OPEN BIOLOGY

rsob.royalsocietypublishing.org

Research

Cite this article: Oshima-Takago T, Takago H. 2017 NMDA receptor-dependent presynaptic inhibition at the calyx of Held synapse of rat pups. *Open Biol.* **7**: 170032.
http://dx.doi.org/10.1098/rsob.170032

Received: 10 February 2017
Accepted: 4 July 2017

Subject Area:
neuroscience

Keywords:
presynaptic NMDA receptor, calcium channel, excitatory postsynaptic current, synapse, glutamate

Author for correspondence:
Hideki Takago
e-mail: takago-hideki@rehab.go.jp

Electronic supplementary material is available online at https://dx.doi.org/10.6084/m9.figshare.c.3827938.

THE ROYAL SOCIETY PUBLISHING

NMDA receptor-dependent presynaptic inhibition at the calyx of Held synapse of rat pups

Tomoko Oshima-Takago[1,2] and Hideki Takago[1,2,3]

[1]Department of Rehabilitation for Sensory Functions, Research Institute, National Rehabilitation Center for Persons with Disabilities, Saitama 359-8555, Japan
[2]Department of Neurophysiology, University of Tokyo Graduate School of Medicine, Tokyo 113-0033, Japan
[3]Department of Otolaryngology, Tokyo Medical and Dental University Graduate School, Tokyo 113-8510, Japan

TO-T, 0000-0003-2698-2631; HT, 0000-0003-2875-4667

N-Methyl-D-aspartate receptors (NMDARs) play diverse roles in synaptic transmission, synaptic plasticity, neuronal development and neurological diseases. In addition to their postsynaptic expression, NMDARs are also expressed in presynaptic terminals at some central synapses, and their activation modulates transmitter release. However, the regulatory mechanisms of NMDAR-dependent synaptic transmission remain largely unknown. In the present study, we demonstrated that activation of NMDARs in a nerve terminal at a central glutamatergic synapse inhibits presynaptic Ca^{2+} currents (I_{Ca}) in a GluN2C/2D subunit-dependent manner, thereby decreasing nerve-evoked excitatory postsynaptic currents. Neither presynaptically loaded fast Ca^{2+} chelator BAPTA nor non-hydrolysable GTP analogue GTPγS affected NMDAR-mediated I_{Ca} inhibition. In the presence of a glutamate uptake blocker, the decline in I_{Ca} amplitude evoked by repetitive depolarizing pulses at 20 Hz was attenuated by an NMDAR competitive antagonist, suggesting that endogenous glutamate has a potential to activate presynaptic NMDARs. Moreover, NMDA-induced inward currents at a negative holding potential (−80 mV) were abolished by intra-terminal loading of the NMDAR open channel blocker MK-801, indicating functional expression of presynaptic NMDARs. We conclude that presynaptic NMDARs can attenuate glutamate release by inhibiting voltage-gated Ca^{2+} channels at a relay synapse in the immature rat auditory brainstem.

1. Introduction

The *N*-methyl-D-aspartate receptor (NMDAR), a member of the ionotropic glutamate receptor family, consists of glycine-binding GluN1 (formerly NR1) subunits together with glutamate-binding GluN2 (GluN2A–D, formerly NR2A–D) subunits and/or glycine-binding GluN3 (GluN3A,B, formerly NR3A,B) subunits, which form a heteromeric receptor complex [1,2]. Postsynaptic NMDARs show variable functions in synaptic transmission, synaptic plasticity, neuronal development and neuronal diseases (for review see [3–7]). Interestingly, over the past two decades, accumulating evidence has indicated that NMDARs are also presynaptically expressed in the cerebral cortex [8–12], hippocampus [13,14], amygdala [15], cerebellum [16–18] and spinal cord [19,20]. Activation of presynaptic NMDARs enhances spontaneous release at glutamatergic synapses in the cerebral cortex [10,21–23], hippocampus [14,24] and amygdala [25] as well as at GABAergic synapses in the cerebellum [18,26–30] and hippocampus [31]. Further, presynaptic NMDAR activation facilitates action potential-evoked glutamate release at cortical [21,22] and hippocampal [32] synapses, and induces long-term potentiation at glutamatergic synapses in the amygdala [33] and subiculum [34,35]. In contrast, previous

research has also indicated that presynaptic NMDARs attenuate action potential-evoked transmitter release at both excitatory [36] and inhibitory [26,28] synapses, and mediate long-term depression of excitatory [10,17,22,37–39] and inhibitory [40] synaptic transmission. However, the mechanisms underlying presynaptic NMDAR-mediated regulation of synaptic transmission remains to be clarified.

Despite these findings, recent studies have challenged the existence of axonal/presynaptic NMDA receptors. In a previous study, focal iontophoretic application of the NMDAR agonist L-aspartate onto the axons of cerebellar stellate cells failed to elicit Ca^{2+} transients in axonal varicosities. However, L-aspartate application onto the dendrites of these cells elicited Ca^{2+} transients in axonal varicosities via opening of voltage-gated Ca^{2+} channels (VGCCs) triggered by passive propagation of depolarization from somatodendritic sites down along axons [41]. Subsequent studies by the same research group revealed no evidence of functional NMDAR expression in the axons of L5 pyramidal cells in the visual cortex [42], or basket cells in the cerebellum [43]. Given such controversial findings, presynaptic recordings should be used to explore whether other types of cells in the CNS exhibit axonal/presynaptic NMDAR expression.

At the calyx of Held synapse in the rat auditory brainstem, whose presynaptic structure is large enough to enable direct whole-cell patch-clamp recordings, application of exogenous L-glutamate inhibits nerve-evoked release of the endogenous neurotransmitter glutamate [44]. This presynaptic inhibitory action is mediated by metabotropic glutamate receptors (mGluRs) [45] and also by α-amino-3-hydroxy-5-methyl-4-isoxazolepropionic acid receptors (AMPARs) [44] expressed in the presynaptic terminal. Both types of glutamate receptors inhibit VGCCs via the activation of heterotrimeric G proteins. However, mGluR and AMPA/kainate receptor antagonists only partially impair the inhibitory effect of L-glutamate on presynaptic Ca^{2+} currents (I_{Ca}), suggesting the involvement of additional mechanisms. In the present study, we show that activation of presynaptic NMDARs induces inward currents at a negative holding potential, inhibits I_{Ca} and decreases action potential-dependent excitatory postsynaptic currents (EPSCs) at the calyx of Held synapse in the immature rat brainstem.

2. Material and methods

2.1. Animals, preparations and solutions

Wistar rats (7–9 days old) of either sex were used. After decapitation under deep isoflurane or halothane inhalation anaesthesia, the brain was quickly removed. Transverse brainstem slices (200–250 µm in thickness) containing the medial nucleus of trapezoid body (MNTB) were cut ice-cold using a tissue slicer (PRO-7, Dosaka, Kyoto, Japan or VT-1200S, Leica, Mannheim, Germany) as described previously [46]. Slices were incubated at 37°C for 30 min and subsequently maintained at room temperature (21–25°C) in artificial cerebrospinal fluid (aCSF) containing (in mM): 125 NaCl, 2.5 KCl, 26 $NaHCO_3$, 1.25 NaH_2PO_4, 2 $CaCl_2$, 1 $MgCl_2$, 10 D-glucose, 3 myo-inositol, 2 sodium pyruvate and 0.5 sodium ascorbate (pH 7.4 when bubbled with 95% O_2 and 5% CO_2). Calyces and MNTB neurons were visualized with a 60× water immersion objective lens (Olympus, Tokyo, Japan) attached to an upright microscope (BX51WI, Olympus, Tokyo, Japan or Axioskop, Zeiss, Oberkochen, Germany). For recording presynaptic Ca^{2+} currents (I_{Ca}), the aCSF additionally contained tetrodotoxin (TTX, 1 µM, Wako, Osaka, Japan) plus tetraethylammonium chloride (TEACl, 10 mM; equimolar replacement for NaCl), and the presynaptic pipette solution contained (in mM): 110 CsCl, 10 TEACl, 40 HEPES, 0.5 EGTA, 1 $MgCl_2$, 12 Na_2 phosphocreatine, 2 ATP-Mg and 0.5 GTP-Na (pH 7.3 with CsOH, 295–305 mOsm kg^{-1}). For recording presynaptic Ba^{2+} currents (I_{Ba}), $CaCl_2$ (2 mM) in the aCSF was replaced with equimolar $BaCl_2$. For recording presynaptic membrane currents, the aCSF additionally contained TTX (1 µM), and the presynaptic pipette solution contained (in mM): 97.5 potassium gluconate, 32.5 KCl, 10 HEPES, 5 EGTA, 1 $MgCl_2$, 12 Na_2 phosphocreatine, 2 ATP-Mg and 0.5 GTP-Na (pH 7.3 with KOH, 295–305 mOsm kg^{-1}). For recording EPSCs) the aCSF routinely contained bicuculline methiodide (10 µM, Sigma, St. Louis, MO, USA) and strychnine hydrochloride (0.5 µM, Sigma) to block GABAergic and glycinergic inhibitory synaptic currents, respectively. The postsynaptic pipette solution contained (in mM): 110 CsF, 30 CsCl, 10 HEPES, 5 EGTA, and 1 $MgCl_2$ (pH adjusted to 7.3 with CsOH, 295–305 mOsm kg^{-1}). Further, *N*-(2,6-diethylphenylcarbamoylmethyl)-triethyl-ammonium chloride (QX314, 5 mM, Alomone Labs, Jerusalem, Israel) was also included in the postsynaptic pipette solution to block action potential generation.

2.2. Chemical compounds

In addition to chemicals already mentioned above, we used the following NMDAR agonists: NMDA from Sigma and (3-chlorophenyl) [3,4-dihydro-6,7-dimethoxy-1-[(4-methoxyphenoxy)methyl]-2(1H)-isoquinolinyl]methanone (CIQ) from Tocris Bioscience (Bristol, UK). We also used the following NMDAR antagonists: 7-chlorokynurenate (7-ClK), D-(−)-2-amino-5-phosphonopentanic acid (D-AP5), 4-(5-(4-bromophenyl)-3-(6-methyl-2-oxo-4-phenyl-1,2-dihydroquinolin-3-yl)-4,5-dihydro-1H-pyrazol-1-yl)-4-oxobutanoic acid (DQP 1105), and (R,S)-α-(4-hydroxyphenyl)-β-methyl-4-(phenylmethyl)-1-piperidinepropanol (Ro 25-6981) from Tocris Bioscience as well as (+)-5-methyl-10,11-dihydro-5H-dibenzo[a,d]cyclohepten-5,10-imine maleate (MK-801) and $ZnCl_2$ from Sigma. Other than NMDAR agonists/antagonists, we used DL-threo-β-benzyloxyaspartic acid (DL-TBOA) from Tocris Bioscience, BAPTA from Dojindo (Kumamoto, Japan), and tricine from Nacalai Tesque (Kyoto, Japan). We obtained all of remaining chemicals used in this study from Sigma.

2.3. Electrophysiological recordings

Whole-cell patch-clamp recordings were made from presynaptic calyceal nerve terminals or postsynaptic MNTB principal neurons. For recording I_{Ca} and I_{Ba}, calyces were voltage-clamped at a holding potential of −80 mV, and depolarizing voltage steps (duration: 3 ms) were applied every 20 s. The I_{Ca} amplitude was measured 2–3 ms after the onset of depolarizing pulses. For recording evoked EPSCs, MNTB neurons were voltage-clamped at a holding potential of −70 mV, and presynaptic axons were stimulated every 20 s by using a tungsten bipolar electrode positioned halfway between the midline and the MNTB. The EPSC

amplitude was measured at their peaks. For presynaptic recordings, the electrode resistance was 4–8 MΩ, and the access resistance was 5–18 MΩ with its compensation by 80%. Leak currents in presynaptic recordings were subtracted by the scaled pulse (P/8) protocol. For postsynaptic recordings, the electrode resistance was 2.5–4 MΩ, and access resistance was 5–15 MΩ with its compensation by 70%. Voltage-clamp recordings were made using a patch-clamp amplifier (Axopatch-200B, Axon Instruments, Foster City, CA, USA). Current-clamp recordings of presynaptic action potentials were made using another patch-clamp amplifier (MultiClamp 700A, Axon Instruments) equipped with a high input impedance (10^{11} Ω) voltage follower. Recorded signals were low-pass-filtered at 5 kHz and digitized at 20–50 kHz by an analogue–digital converter (Digidata 1322A, Axon Instruments) with pCLAMP 9 software (Axon Instruments). Liquid–junction potentials between the pipette solutions and the aCSF were not corrected for. Drugs were bath-applied by switching superfusates using a peristaltic pump or a gravity-fed perfusion system (perfusion rate, 2.0–6.0 ml min^{-1}). Experiments were carried out at room temperature (21–25°C).

2.4. Statistical analysis

Data are presented as mean ± s.e.m.. For comparison of paired data from one group, we first used Shapiro–Wilk normality test, then employed Student's paired *t*-test. For comparison of data from the control groups and groups with various kinds of manipulations such as extracellular/intracellular application of NMDAR agonists/antagonists, we first used Shapiro–Wilk normality test, then employed Student's unpaired *t*-test. Since all the data in this study passed the normality test, nonparametric statistical analysis was not necessary. Unless otherwise described, Student's unpaired *t*-test was employed. Statistical significance was considered when *p*-value was less than 0.05 (SigmaPlot 12.0, Systat Software Inc., San Jose, CA, USA), and significance level is denoted using asterisks ($*p < 0.05$, $**p < 0.01$ and $***p < 0.001$).

3. Results

3.1. Inhibitory effect of NMDA on presynaptic Ca^{2+} currents (I_{Ca})

Previous studies have revealed that activation of mGluRs [45] or AMPARs [44] in the calyx of Held presynaptic terminal inhibits I_{Ca}. First, we investigated whether NMDA also inhibits I_{Ca}. As illustrated in figure 1*a*, bath-application of NMDA (50 μM) in Mg^{2+}-free aCSF inhibited I_{Ca} by 8.3 ± 2.7% at 0 mV ($n = 5$) without a clear shift in the current–voltage relationship (figure 1*b*). The inhibitory effect of NMDA on I_{Ca} was concentration-dependent with an IC_{50} of 135 μM (figure 1*c*). Based on this result, we used a relatively high concentration of NMDA (500 μM) for controls in order to securely analyse the property of NMDA-induced I_{Ca} inhibition. As illustrated in figure 1*d*, bath-application of NMDA at this concentration in Mg^{2+}-free aCSF more evidently inhibited I_{Ca} by 26.0 ± 3.7% at 0 mV ($n = 5$), again without a clear shift in the current–voltage relationship (figure 1*e*). The NMDAR competitive antagonist D-AP5 (500 μM) abolished this NMDA effect (to 1.2 ± 0.9%, $n = 5$, $***p < 0.001$; figure 1*f*,*i*). Although glycine (10 μM) had no effect on NMDA-induced I_{Ca} inhibition (29.9 ± 2.8%, $n = 5$, $p = 0.222$), the NMDAR glycine-site blocker 7-chlorokynurenic acid (7-ClK, 100 μM) blocked it (to 2.8 ± 0.3%, $n = 4$, $***p < 0.001$; figure 1*i*), suggesting that glycine sites of NMDARs may be saturated by endogenous ligand(s) in slices. Surprisingly, a physiological concentration of extracellular Mg^{2+} (1 mM) did not significantly weaken NMDA-induced I_{Ca} inhibition (19.7 ± 1.6%, $n = 5$, $p = 0.158$; figure 1*h*,*i*), although a higher concentration of extracellular Mg^{2+} (5 mM) successfully abolished the inhibition (to 3.6 ± 1.1%, $n = 4$, $**p < 0.01$; figure 1*i*). These results indicate that NMDA-induced I_{Ca} inhibition was indeed mediated by NMDARs. To exclude the possibility that NMDARs expressed in surrounding neurons and/or glia might mediate this NMDA effect, we loaded the NMDAR open channel blocker MK-801 (500 μM) directly into the calyceal nerve terminal through a whole-cell patch pipette. We set the concentration of intra-terminal MK-801 to a range of sub-millimolar based on the procedure used in a previous study, in which MK-801 (1 mM) was applied into presynaptic neurons through the patch pipettes [38]. Under this condition, intra-terminal MK-801 nearly abolished NMDA-induced I_{Ca} inhibition (to 7.3 ± 2.4%, $n = 4$, $**p < 0.01$; figure 1*g*,*i*), suggesting that functional NMDARs are expressed in calyceal nerve terminals, and that their activation inhibits presynaptic VGCCs.

3.2. Subunit dependence of NMDAR-mediated I_{Ca} inhibition

We next investigated which NMDAR subunits contribute to NMDA-induced inhibition of presynaptic VGCCs. Since sub-micromolar concentrations of Zn^{2+} selectively blocks the GluN2A subunit [47], we examined the effect of Zn^{2+} on NMDA-induced I_{Ca} inhibition. In the presence of 300 nM of free Zn^{2+} in the superfusate, which was achieved by a combination of $ZnCl_2$ (27 μM) and zinc buffer tricine (10 mM), NMDA (500 μM) still inhibited I_{Ca} to a similar extent as the control (24.6 ± 3.2%, $n = 4$, $p = 0.792$; figure 2*a*,*d*). For the GluN2B subunit, we used the GluN2B selective antagonist Ro 25-6981 (1 μM) and found no significant difference compared with the control (23.8 ± 3.7%, $n = 4$, $p = 0.690$; figure 2*b*,*d*). In contrast, the GluN2C/2D selective antagonist DQP 1105 (10 μM) significantly weakened the NMDA-induced I_{Ca} inhibition (10.7 ± 1.7%, $n = 5$, $**p < 0.01$; figure 2*c*,*d*), whereas the GluN2C/2D selective potentiator CIQ (10 μM) significantly strengthened this inhibition (35.2 ± 1.9%, $n = 6$, $*p < 0.05$; figure 2*d*). We were unable to pharmacologically evaluate the involvement of the GluN3 subunit due to the lack of subunit-specific agonists/antagonists. Taken these results together, GluN2C/2D subunits, but not GluN2A or GluN2B subunits, contribute to NMDAR-mediated inhibition of presynaptic VGCCs at the immature calyx of Held synapse.

3.3. G proteins and Ca^{2+} are dispensable for NMDAR-mediated I_{Ca} inhibition

At the calyx of Held, a variety of presynaptic receptors are coupled to the heterotrimeric G proteins, and direct interaction of Gβγ subunits with presynaptic VGCCs inhibits I_{Ca} as shown for mGluRs [45], $GABA_B$Rs [48,49], noradrenaline

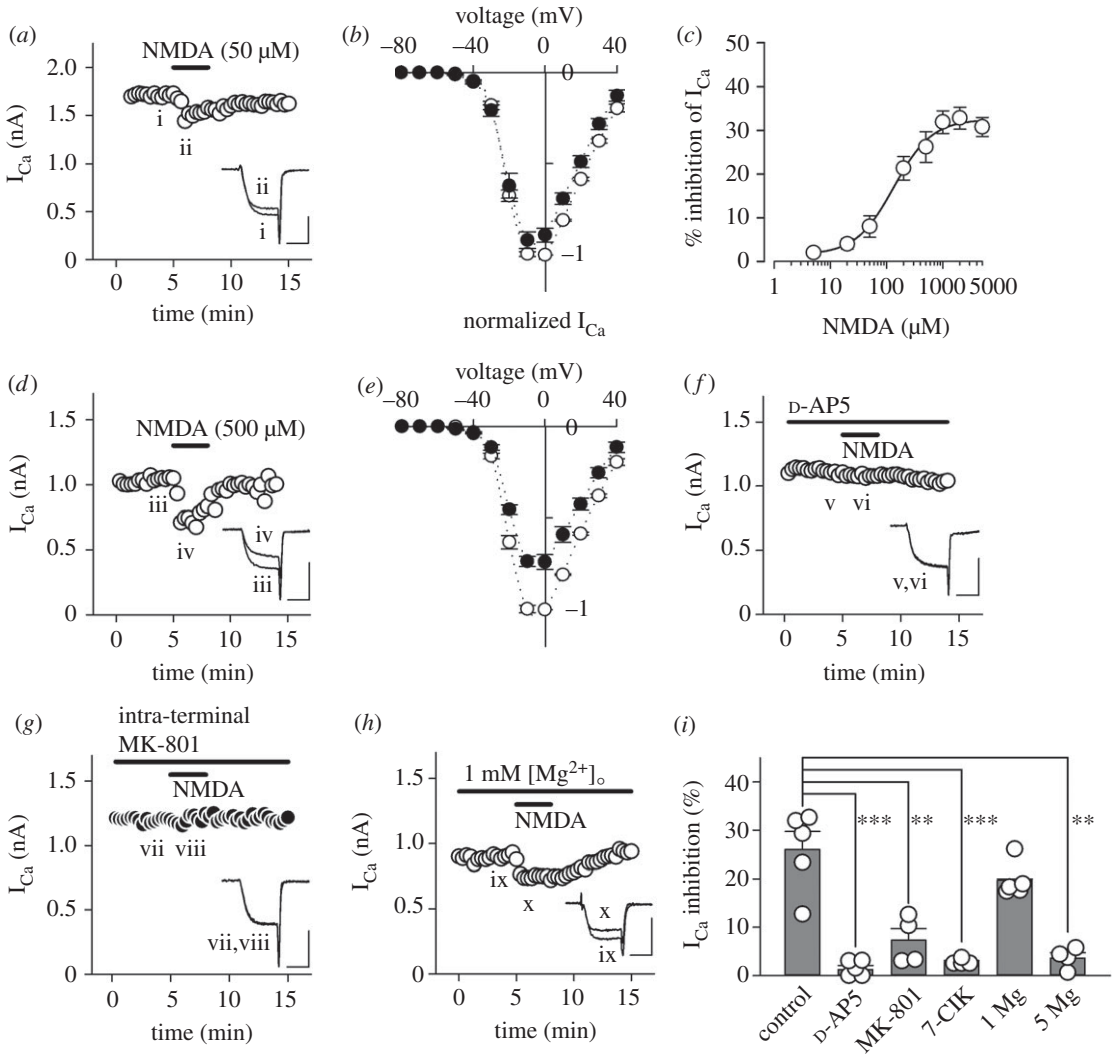

Figure 1. Inhibition of presynaptic Ca^{2+} currents by NMDA. (*a*) NMDA (50 μM) attenuated presynaptic Ca^{2+} currents (I_{Ca}) evoked by a depolarizing pulse (from a holding potential of −80 to 0 mV (duration: 3 ms) in 0 mM Mg^{2+} aCSF. Sample records show I_{Ca} before (i) and during (ii) NMDA application. Three consecutive I_{Ca} were averaged and superimposed for each. (*b*) The current–voltage relationships of I_{Ca} before (open circles) and during (filled circles) 50 μM NMDA application. Mean amplitude of I_{Ca} from 5 calyces at each membrane potential was normalized to that at 0 mV before NMDA application. (*c*) The concentration-dependence of NMDA-induced I_{Ca} inhibition. Individual data points and bars indicate mean ± s.e.m. derived from 4–5 calyces. IC_{50} value was 135 μM. (*d*) I_{Ca} inhibition by NMDA (500 μM) in 0 mM Mg^{2+} aCSF as a control for comparison with that in the presence of NMDAR antagonists. Sample records of I_{Ca} before (iii) and during (iv) NMDA application. (*e*) The current–voltage relationships of I_{Ca} before (open circles) and during (filled circles) 500 μM NMDA application. (*f*) Bath-application of D-AP5 (500 μM) blocked NMDA-induced I_{Ca} inhibition (v,vi). (*g*) MK-801 (500 μM) loaded into the presynaptic terminal nearly abolished NMDA-induced I_{Ca} inhibition (vii,viii). (*h*) Physiological concentration of extracellular Mg^{2+} (1 mM) only weakly attenuated NMDA-induced I_{Ca} inhibition (ix,x). (*i*) Summary of percentage inhibition of I_{Ca} by NMDA (500 μM) in the absence (control, $n = 5$) or presence of the NMDAR blockers such as D-AP5 (500 μM, $n = 5$), intra-terminal MK-801 (iMK-801, 500 μM loaded into presynaptic terminals, $n = 4$) and 7-CIK (100 μM, $n = 4$) as well as those in the presence of Mg^{2+} (1 mM, $n = 5$; 5 mM, $n = 4$). Both individual data (open circles) and mean ± s.e.m. (dark grey bars) are shown. Asterisks indicate significant statistical differences (**$p < 0.01$, ***$p < 0.001$). Scale bars in the superimposed sample traces indicate 2 ms for horizontal and 1 nA for vertical axes, respectively.

α_2Rs [50], adenosine A_1Rs [51], 5-HT_{1B}Rs [52] and AMPARs [44]. To investigate the possibility that this mechanism also underlies NMDA-induced I_{Ca} inhibition, we loaded the non-hydrolysable GTP analogue GTPγS (0.2 mM) into the presynaptic terminal through whole-cell patch pipettes. As GTPγS diffused into a terminal from a presynaptic pipette, I_{Ca} became smaller in amplitude and slower in rise time, consistent with previous studies [48,53]. After the I_{Ca} amplitude had reached a steady level, bath-application of NMDA (500 μM) attenuated I_{Ca} (figure 3*a*,*e*) by 27.5 ± 4.2% ($n = 5$). This magnitude of inhibition in the presence of intra-terminal GTPγS was similar to that observed in its absence ($p = 0.784$), suggesting that NMDAR-mediated I_{Ca} inhibition does not require G proteins. We then sought to confirm that the lack of occlusive effect of intra-terminal GTPγS on NMDA-induced I_{Ca} inhibition was not due to a failure of drug action. Following bath-application of the high affinity group III mGluR agonist L-AP4 (100 μM), significant differences in the magnitude of I_{Ca} inhibition were observed between the absence (22.5 ± 1.6%, $n = 5$) and presence (2.2 ± 1.3%, $n = 5$, ***$p < 0.001$, data not shown) of intra-terminal GTPγS (0.2 mM). Thus, intra-terminal GTPγS securely occluded mGluR-mediated I_{Ca} inhibition. After intra-terminal GTPγS (0.2 mM) had fully activated the mGluR- and AMPAR-mediated I_{Ca} inhibition pathways, we examined whether L-glutamate further inhibits I_{Ca} via the activation of presynaptic NMDARs. As shown in figure 3*b*, bath-application of L-glutamate (500 μM) inhibited

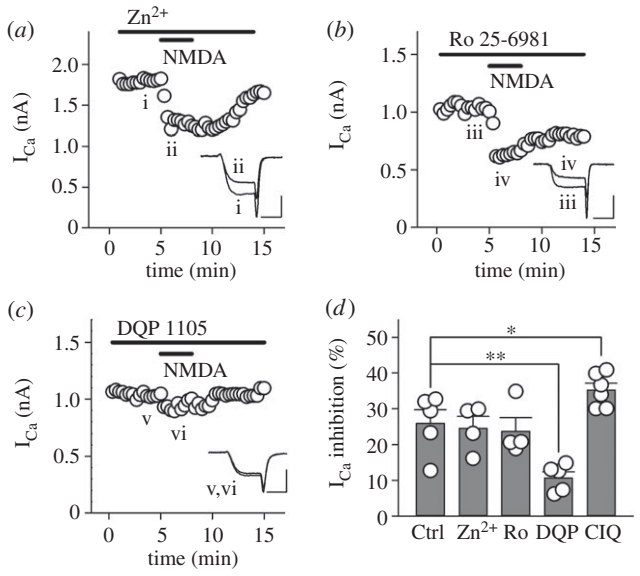

Figure 2. NMDAR-mediated I_{Ca} inhibition is GluN2C/2D-dependent. In each experiment, the bath superfusate additionally contained one of the specific NMDAR subunit antagonists: (*a*) zinc (300 nM as free Zn^{2+}) for GluN2A, (*b*) Ro 25-6981 (1 µM) for GluN2B, and (*c*) DQP 1105 (10 µM) for GluN2C/2D, respectively. (*d*) Summary of NMDAR subunit dependence of I_{Ca} inhibition. Note that a GluN2C/2D potentiator, CIQ (10 µM), augmented NMDAR-mediated I_{Ca} inhibition. Both individual data (open circles) and mean ± s.e.m. (dark grey bars) are shown. Asterisks indicate significant statistical differences (*$p < 0.05$, **$p < 0.01$). Scale bars in the superimposed sample traces indicate 2 ms for horizontal and 1 nA for vertical axes, respectively.

I_{Ca} by 19.4 ± 0.6% ($n = 4$), and this effect was lessened to 6.1 ± 0.9% ($n = 4$, *$p < 0.05$) by a mixture of D-AP5 (500 µM) and 7-ClK (100 µM). These results suggest that presynaptic NMDARs mainly mediate L-glutamate-induced additional I_{Ca} inhibition after full activation of mGluRs and AMPARs [44].

We then examined whether intra-terminal Ca^{2+}, which is elevated by presynaptic NMDAR activation, mediates NMDA-induced I_{Ca} inhibition. The fast Ca^{2+} chelator BAPTA (10 mM) loaded into the calyceal terminal had no effect on NMDA-induced I_{Ca} inhibition (31.1 ± 1.8%, $n = 4$, $p = 0.290$; figure 3*c*,*e*). Moreover, replacement of the VGCC charge carrier Ca^{2+} with Ba^{2+} (2 mM) had no significant effect on the NMDA-induced inhibition of presynaptic Ba^{2+} currents (21.2 ± 1.0%, $n = 5$, $p = 0.254$; figure 3*d*,*e*). These results suggest that intra-terminal Ca^{2+} does not contribute to NMDA-induced I_{Ca} inhibition.

We also examined a possible effect of Na^+ on the I_{Ca} inhibition. When extracellular Na^+ was replaced with equimolar TEA^+, bath-application of NMDA (500 µM) no longer inhibited I_{Ca} (3.5 ± 1.0%, $n = 4$; **$p < 0.01$; figure 3*e*), suggesting that Na^+ influx through presynaptic NMDARs may somehow mediate the I_{Ca} inhibition.

We further aimed to identify the intracellular mechanism(s) that links NMDAR activation and Ca^{2+} channel inhibition in the calyceal terminal. Since presynaptic NMDARs are relevant to nitric oxide synthesis in the cerebellum [54,55] as well as protein kinase C activation in the neocortex [56], we examined whether such chemicals as the nitric oxide synthase inhibitor L-NNA (1 mM) or the protein kinase C inhibitor staurosporine (2 µM) attenuate I_{Ca} inhibition induced by NMDA (500 µM). However, neither agent exerted a significant effect (32.1 ± 3.1%, $n = 4$, $p = 0.259$ for L-NNA; 23.1 ± 2.3%, $n = 4$, $p = 0.560$ for staurosporine, figure 3*e*). Moreover, we examined whether endocannabinoid signalling triggered via the activation of NMDARs in the postsynaptic MNTB neuron is associated with NMDA-induced I_{Ca} inhibition. Based on the protocol in a previous study [57], we performed these experiments using the cannabinoid receptor type 1 blocker AM 251 (5 µM). In the presence of AM 251 in aCSF, NMDA application still inhibited I_{Ca} by 23.6 ± 3.0% ($n = 4$, $p = 0.473$, figure 3*e*), suggesting that endocannabinoid-dependent retrograde signalling is not involved in NMDA-induced I_{Ca} inhibition.

3.4. NMDA-induced currents in the calyceal nerve terminal

We examined whether NMDARs expressed in the calyceal nerve terminal exhibit ionotropic channel properties. In Mg^{2+}-free aCSF containing TTX (1 µM), at a holding potential of −80 mV, bath-application of NMDA (500 µM) induced inward currents (35.5 ± 9.9 pA, $n = 7$, figure 4*a*), which were accompanied by an increase in membrane noise (figure 4*a*). Intra-terminal MK-801 (500 µM) significantly reduced these NMDA currents to 8.9 ± 2.2 pA ($n = 4$; figure 4*b*). After maximal blockade of presynaptic K^+ channels by using a Cs^+-based pipette solution containing TEA (10 mM) and also replacement of extracellular Ca^{2+} with equimolar Ba^{2+} (2 mM), bath-application of NMDA (500 µM) still induced inward currents (17.3 ± 6.9 pA, $n = 5$; figure 4*c*), which were again accompanied by an increase in membrane noise (figure 4*c*). Intra-terminal MK-801 (500 µM) had no effect on the presynaptic resting membrane potential (−60.6 ± 1.2 mV for control, −61.8 ± 1.5 mV for MK-801, $n = 5$ for each, $p = 0.471$), peak amplitude (95.6 ± 2.0 mV for control, 96.8 ± 2.1 mV for MK-801, $p = 0.655$) or half-width (0.49 ± 0.04 ms for control, 0.47 ± 0.07 ms for MK-801, $p = 0.835$) of presynaptic action potentials, suggesting that its blocking effect is specific for NMDARs. These results indicate that functional NMDARs are expressed in the calyceal nerve terminals. The reduction in the inward current amplitude following blockade of K^+ channels and small currents remaining in the presence of intra-terminal MK-801 (figure 4*b*) imply that activation of NMDARs in surrounding cells might additionally contribute to NMDA-induced inward currents via an increase in extracellular K^+ concentration.

3.5. NMDAR-mediated I_{Ca} inhibition by endogenous glutamate

We then investigated whether endogenous glutamate inhibits I_{Ca} via the activation of presynaptic NMDARs. When I_{Ca} were evoked by a train of 30 depolarizing pulses (to 0 mV, duration: 1 ms) at 20 Hz, the I_{Ca} amplitude displayed an activity-dependent decline, and reached a steady-state (ss) level lower than that of the first I_{Ca} (I_{ss}/I_{1st}: 92.9 ± 4.0%, $n = 5$). Previous research reported that elevated extracellular glutamate by repetitive depolarizing stimuli activates presynaptic mGluRs, thereby reducing glutamate release [58]. This mechanism may have partly contributed to the I_{Ca} decline that we observed in this experiment. In the presence of D-AP5 (500 µM) in aCSF, no changes in this I_{Ca} decline were observed (I_{ss}/I_{1st}: 92.6 ± 4.3%, $n = 5$,

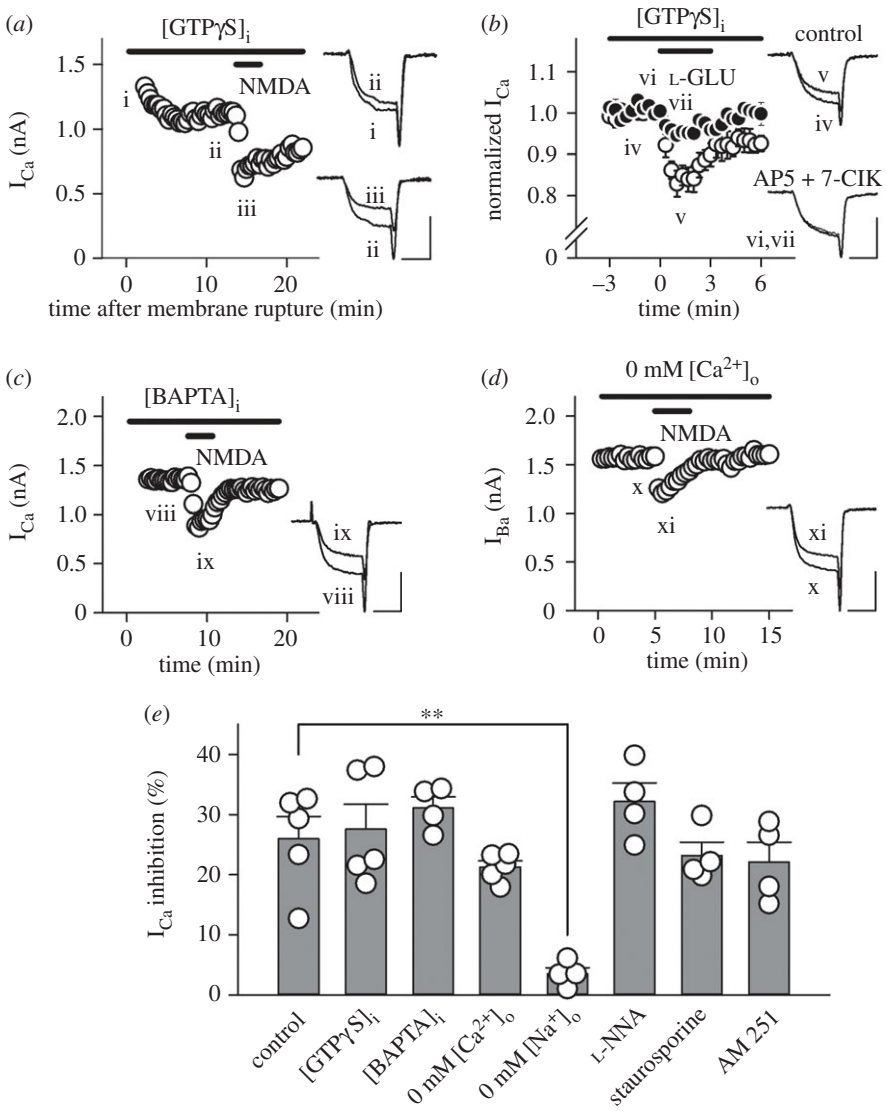

Figure 3. NMDAR-mediated I_{Ca} inhibition requires neither G proteins nor Ca^{2+}. (*a*) Intra-terminal loading of GTPγS (0.2 mM) attenuated I_{Ca} (i,ii), but had no effect on NMDA-induced I_{Ca} inhibition (iii). (*b*) In the presence of GTPγS (0.2 mM), L-glutamate (500 μM) inhibited I_{Ca} (open circles, iv,v, $n = 4$). A cocktail of NMDAR blockers (500 μM D-AP5 plus 100 μM 7-CIK) weakened the L-glutamate-induced I_{Ca} inhibition (filled circles, vi,vii, $n = 4$). (*c*) NMDA (500 μM) attenuated I_{Ca} (viii, ix) in the presence of BAPTA (10 mM) in the presynaptic terminal. (*d*) NMDA (500 μM) attenuated I_{Ba} (x,xi) through presynaptic Ca^{2+} channels. I_{Ba} was evoked by a depolarizing pulse to 0 mV (duration: 3 ms). Scale bars in the superimposed sample traces indicate 2 ms for horizontal and 1 nA for vertical axes, respectively. (*e*) Summary of percentage inhibition of I_{Ca} by NMDA (500 μM) in the absence (control, $n = 5$) or presence of the various agents to explore a candidate intracellular mechanism(s) which underlies NMDAR-mediated I_{Ca} inhibition. In addition to intra-terminal GTPγS ($[GTPγS]_i$, $n = 5$) and BAPTA ($[BAPTA]_i$, $n = 4$) as well as replacement of extracellular Ca^{2+} with Ba^{2+} (0 mM $[Ca^{2+}]_o$, $n = 5$), omission of extracellular Na (0 mM $[Na^+]_o$, $n = 4$), nitric oxide synthesis inhibitor L-NNA (1 mM, $n = 4$), protein kinase C inhibitor staurosporine (2 μM, $n = 4$), and cannabinoid receptor type 1 inhibitor AM 251 (5 μM, $n = 4$) were tested. Asterisks indicate a significant statistical difference (**$p < 0.01$).

$p = 0.615$, Student's paired *t*-test, figure 5*a*). In contrast, when I_{Ca} were evoked by a train at a higher-frequency of 200 Hz, the I_{Ca} amplitude displayed activity-dependent facilitation as previously reported for rats [59] and for mice [60]. Under this condition, D-AP5 again failed to alter the magnitude of facilitation (I_{ss}/I_{1st}: 117.0 ± 2.2% for control, 118.6 ± 1.6% for D-AP5, $n = 5$, $p = 0.536$, Student's paired *t*-test, figure 5*b*).

Further, to clarify whether endogenous glutamate activates presynaptic NMDARs, I_{Ca} were evoked by a train at 20 Hz in the presence of the glutamate uptake blocker TBOA (100 μM) in aCSF. As observed in the absence of TBOA, the I_{Ca} amplitude displayed activity-dependent decline and reached a steady-state level lower than that of the first I_{Ca} (I_{ss}/I_{1st}: 86.4 ± 2.8%, $n = 7$). Previous studies already revealed that not only repetitive depolarizing stimuli [58] but also glutamate transporter blockade by TBOA [61] raises extracellular glutamate, thereby activating presynaptic mGluR-dependent autoinhibition of glutamate release. Both mechanisms may have partly contributed to the I_{Ca} decline that we observed with this protocol. Under this condition, bath-application of D-AP5 (500 μM) significantly weakened this magnitude of I_{Ca} decline (I_{ss}/I_{1st}: 90.3 ± 1.6%, $p < 0.05$, figure 5*c*). These results imply that endogenous glutamate released from the nerve terminal or surrounding cells [14,62] inhibits I_{Ca} via the activation of presynaptic NMDARs. Furthermore, these results suggest that NMDAR-mediated presynaptic inhibition may not occur under physiological conditions, in which extracellular glutamate is promptly cleared by glial uptake systems. However, this inhibition may occur under pathological conditions, in which extracellular glutamate concentration rises to a high level.

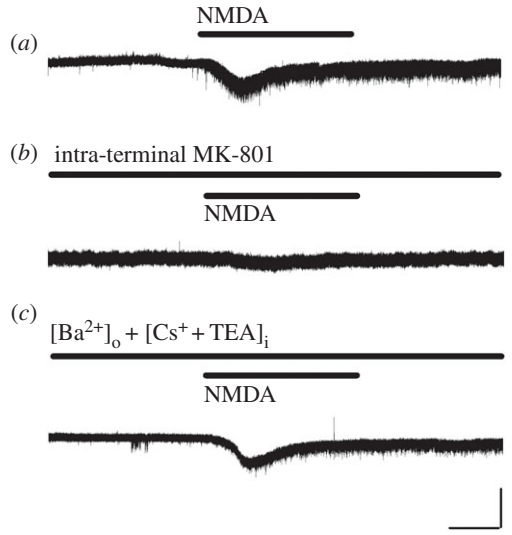

Figure 4. NMDA-induced currents in calyceal nerve terminals. (*a*) Bath-application of NMDA (500 µM) induced inward currents at a holding potential of −80 mV, with concomitant increase in membrane noise. (*b*) Intra-terminal MK-801 (500 µM) blocked the NMDA currents. (*c*) In the presence of intra-terminal Cs^+ (110 mM) as well as TEA (10 mM) and Ba^{2+} (2 mM, substituted for Ca^{2+}) in aCSF, NMDA (500 µM) induced significant inward currents, again with concomitant increase in membrane noise. Data are obtained in Mg^{2+}-free aCSF. Scale bars in the superimposed sample traces indicate 1 min for horizontal and 20 pA for vertical axes, respectively.

3.6. Reduction of evoked AMPA-EPSC amplitude by NMDA

Finally, we examined whether NMDA has an inhibitory effect on glutamatergic postsynaptic currents recorded from MNTB neurons. To abolish postsynaptic NMDA action, the NMDAR open channel blocker MK-801 (5 mM) was applied into MNTB neurons through postsynaptic patch pipettes in aCSF containing Mg^{2+} (1 mM). We set the concentration of intracellular MK-801 to 5 mM in accordance with procedures described in previous studies, which used 5 mM [24], 4 and 1 mM [39], 2 mM [14], or 1 mM [38,63,64] of intracellular MK-801. The selected concentration in this experiment was 10 times higher than that used for presynaptic recordings (500 µM) in order to ensure maximal blockade of postsynaptic NMDARs. Under this condition, bath-application of NMDA (500 µM) attenuated evoked AMPA-EPSCs (figure 6*a*) by 32.9 ± 1.4% ($n = 7$) with minimal change in holding currents in MNTB neurons (96.5 ± 38.0 pA at −70 mV). As shown in NMDA-induced I_{Ca} inhibition (figure 1*f*,*i*), the NMDAR competitive antagonist D-AP5 blocked NMDA-induced EPSC reduction (to 2.4 ± 1.4%, $n = 4$, $p < 0.05$, figure 6*b*). The inhibitory effect of NMDA on evoked AMPA-EPSCs was concentration-dependent with an IC_{50} of 112 µM (figure 6*c*). In the paired-pulse stimulation protocol with an inter-pulse interval of 20 ms, NMDA (500 µM) increased the paired-pulse ratio (PPR, the ratio of second amplitude to the first) of AMPA-EPSCs by 28.7 ± 2.6% ($n = 7$, ***$p < 0.001$, Student's paired *t*-test; figure 6*d*). Thus, this finding confirmed that NMDA application indeed decreases evoked AMPA-EPSCs by means of a presynaptic mechanism.

Moreover, we examined whether tonic activation of presynaptic NMDAR by endogenous glutamate alters basic synaptic transmission. Bath-application of the NMDAR competitive blocker D-AP5 (500 µM) altered neither amplitude (100.5 ± 1.8% of control, $n = 4$, $p = 0.829$, figure 6*e*) nor PPR (96.9 ± 1.9% of control, $n = 4$, $p = 0.252$, Student's paired *t*-test, figure 6*f*) of evoked AMPA-EPSCs, suggesting that presynaptic NMDARs are not tonically activated to reduce action potential-dependent release.

4. Discussion

In the present study, we demonstrated that activation of GluN2C/2D subunit-containing presynaptic NMDARs inhibits VGCCs, thereby attenuating action potential-driven release at a central glutamatergic synapse of young rats. Furthermore, we successfully recorded NMDA-induced currents using presynaptic voltage-clamp recordings, confirming functional expression of presynaptic NMDARs at this synapse.

Presynaptic inhibitory effects of NMDAR activation on nerve-evoked synaptic currents were reported at inhibitory synapses in the cerebellum [26,28] as well as excitatory synapses in the spinal cord primary afferents [36]. These studies reported a weak blocking effect of Mg^{2+} on NMDAR-mediated presynaptic inhibition, indicating that GluN2C/2D (preferentially GluN2D) subunits may be involved. In the present study, we also observed a weak blocking effect of Mg^{2+} on NMDAR-mediated I_{Ca} inhibition (figure 1*g*,*h*). Further, we confirmed that the GluN2C/2D selective antagonist DQP 1105 weakened (figure 2*c*,*d*) but the GluN2C/2D selective potentiator CIQ strengthened NMDAR-mediated I_{Ca} inhibition (figure 2*d*). Postsynaptic MNTB neurons before the onset of hearing employ GluN2A/2B subunit-containing NMDARs [65], whereas presynaptic calyceal terminals use GluN2C/2D subunit-containing NMDARs (figure 2*c*,*d*). Thus, NMDA induced the GluN2C/2D-dependent I_{Ca} inhibition, which may decrease the action potential-driven glutamate release, resulting in the reduction of evoked EPSCs (figure 6*a*). Notably, presynaptic NMDAR activation still inhibited VGCCs (figure 1*h*,*i*) and glutamate release (figure 6*a*) in the presence of a physiological concentration of Mg^{2+} (1 mM) in aCSF, where postsynaptic NMDARs are blocked at resting membrane potential. It is also noteworthy that postsynaptic MNTB neurons predominantly employ GluN2A/2C subunit-containing NMDARs after the onset of hearing [66].

At some other synapses, activation of presynaptic NMDARs enhances nerve-evoked transmitter release [23,67]. Whereas tonic elevation of intra-terminal Ca^{2+} facilitates transmitter release, it potentially inhibits nerve-evoked transmitter release via adaptation of Ca^{2+} sensor for exocytosis [68]. At the calyx of Held, however, either intra-terminal BAPTA (10 mM) or replacement of the charge carrier Ca^{2+} with Ba^{2+} had no effect on NMDA-induced I_{Ca} inhibition. This excludes the involvement of Ca^{2+}-dependent intracellular mechanism(s). Sustained depolarization of the nerve terminal upon NMDA application may inhibit evoked transmitter release by reducing the amplitude of presynaptic action potential. However, this was not the case for NMDAR-mediated presynaptic inhibition in the present study. Expected presynaptic depolarization from the inward currents produced by NMDA (less than 50 pA) is less than 10 mV [44]. Such a mild depolarization facilitates rather than inhibits transmitter release [69,70] by causing tonic Ca^{2+} entry into the terminal [69]. However, upon activation

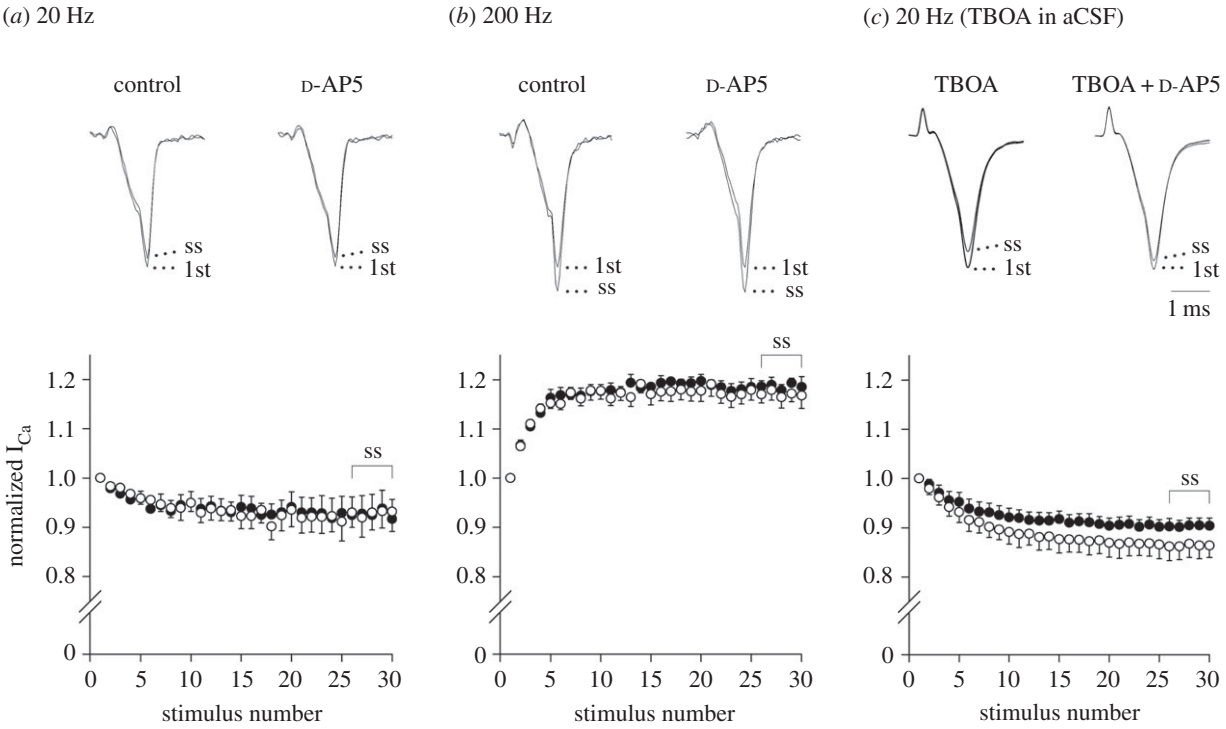

Figure 5. Involvement of endogenous NMDA receptor ligand(s) in activity-dependent decline of I_{Ca}. I_{Ca} were elicited by a train of 30 square depolarizing pulses (to 0 mV, duration: 1 ms). Sample records show the first (1st) and 26th–30th averaged I_{Ca} (ss, superimposed), which are normalized to the first I_{Ca}, in the absence (left traces) or presence (right traces) of D-AP5 (500 μM). Data points and bars represent mean ± s.e.m. of the normalized I_{Ca} amplitude in the presence (filled circles) or absence (open circles) of D-AP5 in the aCSF. (*a*) Activity-dependent decline of I_{Ca} amplitude by 20 Hz stimuli. No significant difference. (*b*) Activity-dependent facilitation of I_{Ca} amplitude by 200 Hz stimuli. No significant difference. (*c*) Activity-dependent decline of I_{Ca} amplitude by 20 Hz stimuli in the presence of the glutamate transporter inhibitor TBOA (100 μM). In the presence of D-AP5, I_{Ca} decline became significantly less ($p < 0.05$, Student's paired *t*-test). A horizontal scale bar in the superimposed sample traces indicates 1 ms.

of presynaptic NMDARs, this facilitatory effect was actually masked by stronger inhibitory effect of presynaptic NMDAR-dependent I_{Ca} inhibition. This effect may have been associated with the smaller reduction in evoked EPSC amplitude (32.9% in 1 mM Mg^{2+} in aCSF, figure 6), compared to the reduction in I_{Ca} amplitude (18.1% in 1 mM Mg^{2+} in aCSF, figure 1*h*,*i*) (cf. the EPSC amplitude is proportional to the fourth power of I_{Ca} [71]). This discrepancy may also be explained by spillover of a millimolar range of MK-801 from the patch pipette during its approach onto the postsynaptic MNTB neuron, which may have partially attenuated presynaptic NMDARs upon the EPSC recording.

Blockade of NMDA-induced I_{Ca} inhibition by loading of intra-terminal MK-801 (figure 1*g*) and by omission of extracellular Na^+ (figure 3*e*) implies that Na^+ influx through presynaptic NMDARs may be involved. Interestingly, Na^+ suppressed the enhancement of spontaneous transmitter release by presynaptic NMDAR activation in the mouse primary visual cortex [56]. The Na^+-mediated regulation mechanism should be elucidated in future studies.

The VGCC in the calyceal terminal is a common target for presynaptic G protein-coupled receptors (GPCRs), including mGluRs [45], $GABA_B$Rs [48,72], noradrenaline α_2Rs [50], adenosine A_1Rs [51] and 5-HT_{1B}Rs [52] as well as presynaptic AMPARs [44]. These receptors activate heterotrimeric G proteins, and direct interaction of Gβγ subunits with presynaptic Ca^{2+} channels inhibits I_{Ca} [49]. These presynaptic inhibitory effects of GPCR ligands on VGCCs occlude with each other [51] and are blocked by the non-hydrolysable GTP analogue GTPγS loaded into the calyceal terminal [49], implying that they share the same pathway. However, the present study showed intra-terminal GTPγS had no effect on NMDA-induced I_{Ca} inhibition. This suggests that the mechanism which links NMDARs to VGCCs is distinct from the common GTP-G protein pathway.

Then, we aimed to identify the intracellular mechanism(s) to connect NMDAR activation to VGCC inhibition in the calyceal nerve terminal using the nitric oxide synthase inhibitor L-NNA, the protein kinase C inhibitor staurosporine and the CBR1 inhibitor AM 251. However, none of these inhibitors weakened NMDA-induced I_{Ca} inhibition. Thus, future studies to determine the candidate intracellular mechanism(s) are needed.

Some pieces of evidence in the present study demonstrate functional expression of NMDARs in calyceal nerve terminals rather than in surrounding cells. First, NMDA-induced inward currents were recorded in the calyceal terminal following blockade of potassium conductance (figure 4*c*). Second, loading of MK-801 into the nerve terminal blocked NMDA-induced inhibition of I_{Ca} (figure 1*g*) and NMDA-induced inward currents (figure 4*b*), whereas NMDA-induced presynaptic inhibition was observed in the presence of MK-801 in postsynaptic MNTB cells (figure 6*a*). Third, after replacement of extracellular Ca^{2+} with Ba^{2+}, NMDA inhibited presynaptic Ba^{2+} currents (figure 3*d*), despite the fact that synaptic transmission is nearly terminated after replacement of Ca^{2+} with Ba^{2+} [44]. Unfortunately, the extremely low amplitude of NMDA-induced presynaptic membrane currents (17.3 pA at −80 mV, figure 5*c*) prevented us from further dissecting the properties of NMDARs expressed in calyceal terminals.

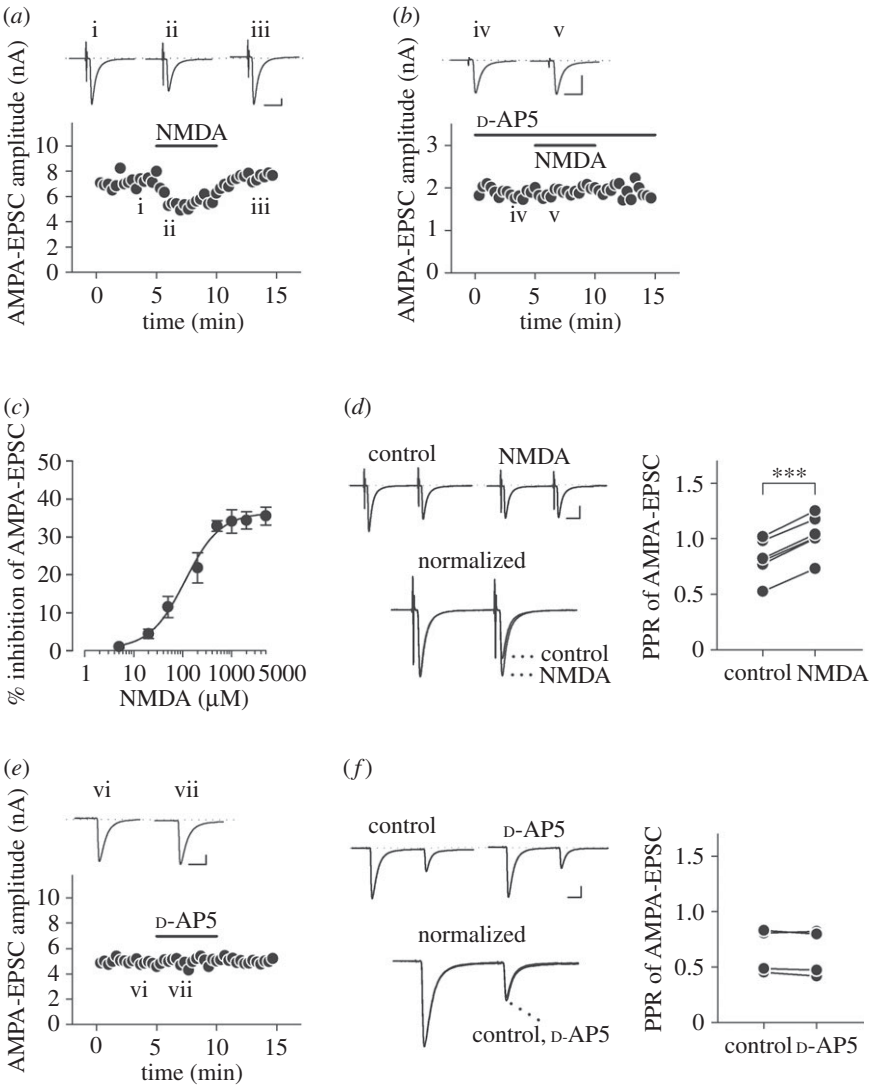

Figure 6. Attenuation of glutamate release by NMDA. (*a*) Inhibition of evoked AMPA-EPSCs by NMDA (500 μM) in the presence of Mg^{2+} (1 mM) in aCSF and MK-801 (5 mM) in an MNTB neuron. Note that the concentration of postsynaptically loaded MK-801 (5 mM) was 10 times higher than that of presynaptically loaded MK-801 (500 μM, figure 1) for maximal block of postsynaptic NMDARs. Sample records show AMPA-EPSCs before (i) and during (ii) bath-application of NMDA (500 μM), and after washout (iii). Three consecutive EPSCs were averaged and superimposed for each. (*b*) Bath-application of D-AP5 (500 μM) blocked the inhibitory effect of NMDA on evoked AMPA-EPSCs (iv,v). (*c*) The concentration-dependence of NMDA-induced evoked AMPA-EPSC inhibition. Individual data points and bars indicate mean ± s.e.m. derived from 4 to 7 neurons. IC_{50} value was 112 μM. (*d*) AMPA-EPSCs evoked by paired-pulse stimulation (inter-pulse interval: 20 ms) in the presence of intracellular MK-801 (5 mM). Sample records in the upper panel show AMPA-EPSCs before (control) and during NMDA application (NMDA). Those in the bottom panel show EPSCs normalized to the first amplitude, in the presence and absence of NMDA (500 μM) (superimposed). Plots on the right panel indicate PPRs before and after NMDA application in 7 neurons. NMDA significantly increased the PPR of AMPA-EPSCs (***$p < 0.001$, Student's paired *t*-test). (*e*) Bath-application D-AP5 (500 μM) did not alter the amplitude of AMPA-EPSCs. Sample records show AMPA-EPSCs before (vi) and during (vii) its application. (*f*) PPRs were unaffected by D-AP5 application in 4 neurons. No significant difference. Scale bars in the superimposed sample traces indicate 5 ms for horizontal and 1 nA for vertical axes, respectively.

The presynaptic inhibitory effect of NMDA had an IC_{50} of 135 μM for I_{Ca} (figure 1*c*) and 112 μM for evoked EPSCs (figure 6*c*), respectively. The recombinant NMDAR currents in *Xenopus* oocytes have an EC_{50} of 30–60 μM for NMDA, depending on GluN2 subunits co-expressed with the GluN1 subunit [73]. Similarly, the EC_{50} of native NMDAR currents in CA1 neurons in hippocampal slices is 38 μM [74]. The relatively low affinity of presynaptic NMDARs may reflect the involvement of GluN1 splice variants with low ligand affinity [75]. Ambient glutamate concentration is 55 nM at the calyx of Held synapse of immature rats [76]. In hippocampal slices, the glutamate concentration is 30 nM in the absence of the glutamate transporter inhibitor TBOA, but rises to 200 nM in its presence [74,77]. In the synaptic cleft, the glutamate concentration is estimated to rise above 300 μM [78] or up to 1 mM [79] during excitatory transmission. In experimental anoxia, the glutamate concentration in the cerebral cortex can rise to 400 μM *in vivo* [80]. Our finding that D-AP5 affected I_{Ca} evoked by repetitive stimulation in the presence of TBOA, but not in its absence (figure 5), suggests that presynaptic NMDARs do not operate under physiological conditions. However, under pathological conditions in which extracellular glutamate concentration rises to a high level (e.g. brain anoxia), presynaptic NMDARs may act to reduce glutamate release, thereby playing a protective role against neuronal death due to glutamate excitotoxicity.

Previous research reported that synaptic transmission and glutamate transporter activity at the calyx of Held synapse differ between physiological and room temperature [81]. Thus, the temperature-dependency of NMDAR-mediated

presynaptic inhibition remains to be examined in order to further investigate the physiological and pathophysiological relevance. Besides, it needs to be noted that all data in this study were obtained using immature rats (P7–9). It is beyond the scope of our current study to clarify whether the NMDAR-dependent presynaptic inhibition is developmentally regulated, similar to TBOA-induced presynaptic mGluR activation [61].

In conclusion, the present study identified a novel regulatory mechanism for NMDAR-dependent presynaptic inhibition at an excitatory synapse in the auditory brainstem of rat pups by direct presynaptic recordings. Moreover, it also revealed the presence of functional presynaptic NMDARs. These findings bring significant insights to the controversial research field on presynaptic NMDARs. Finally, this study not only provides applicable implications to presynaptic inhibition at other central synapses, but also potentially serves to develop drugs targeting presynaptic NMDARs in the CNS.

Ethics. All experiments complied with the guideline of the Physiological Society of Japan as well as the institutional guidelines. The experimental protocols were approved by the animal experimentation committees of University of Tokyo, Tokyo Medical and Dental University, and National Rehabilitation Center for Persons with Disabilities.

Data accessibility. The datasets supporting this article have been uploaded as part of the electronic supplementary material.

Authors' contributions. T.O.-T. and H.T. designed the study, carried out experiments, analysed the data and wrote the manuscript. Both authors gave final approval for publication.

Competing interests. We have no competing interests.

Funding. This study was supported by JSPS KAKENHI (Grant number 19791196, 25670722 and 16K11204 to H.T. as well as Grant number 16K18374 to T.O.-T.).

Acknowledgements. We thank Drs Tomoyuki Takahashi, Ken Kitamura, Koichi Mori, Kensuke Watanabe, Masanobu Kano, Takayuki Murakoshi, Yoshinori Sahara, Yukihiro Nakamura, Taro Ishikawa, Misa Shimuta, Nobutake Hosoi and Masao Tachibana for comments and/or help.

References

1. Monyer H, Sprengel R, Schoepfer R, Herb A, Higuchi M, Lomeri H, Burnashev N, Sakmann B, Seeburg PH. 1992 Heteromeric NMDA receptors: molecular and functional distinction of subtypes. *Science* **256**, 1217–1221. (doi:10.1126/science.256.5060.1217)
2. Ulbrich MH, Isacoff EY. 2008 Rules of engagement for NMDA receptor subunits. *Proc. Natl Acad. Sci. USA* **105**, 14 163–14 168. (doi:10.1073/pnas.0802075105)
3. Nicoll RA, Kauer JA, Malenka RC. 1988 The current excitement in long-term potentiation. *Neuron* **1**, 97–103. (doi:10.1016/0896-6273(88)90193-6)
4. McBain CJ, Mayer ML. 1994 *N*-Methyl-D-aspartic acid receptor structure and function. *Physiol. Rev.* **74**, 723–760.
5. Collingridge GL, Bliss TV. 1995 Memories of NMDA receptors and LTP. *Trends Neurosci.* **18**, 54–56. (doi:10.1016/0166-2236(95)80016-U)
6. Cull-Candy S, Brickley S, Farrant M. 2001 NMDA receptor subunits: diversity, development and disease. *Curr. Opin. Neurobiol.* **11**, 327–335. (doi:10.1016/S0959-4388(00)00215-4)
7. Lüscher C, Malenka RC. 2012 NMDA receptor-dependent long-term potentiation and long-term depression (LTP/LTD). *Cold. Spring Harb. Perspect. Biol.* **4**, a005710. (doi:10.1101/cshperspect.a005710)
8. Aoki C, Venkatesan C, Go CG, Mong JA, Dawson TM. 1994 Cellular and subcellular localization of NMDA-R1 subunit immunoreactivity in the visual cortex of adult and neonatal rats. *J. Neurosci.* **14**, 5202–5222.
9. DeBiasi S, Minelli A, Melone M, Conti F. 1996 Presynaptic NMDA receptors in the neocortex are both auto- and heteroreceptors. *Neuroreport* **7**, 2773–2776. (doi:10.1097/00001756-199611040-00073)
10. Corlew R, Wang Y, Ghermazien H, Erisir A, Philpot BD. 2007 Developmental switch in the contribution of presynaptic and postsynaptic NMDA receptors to long-term depression. *J. Neurosci.* **27**, 9835–9845. (doi:10.1523/JNEUROSCI.5494-06.2007)
11. Larsen RS *et al.* 2011 NR3A-containing NMDARs promote neurotransmitter release and spike timing-dependent plasticity. *Nat. Neurosci.* **14**, 338–344. (doi:10.1038/nn.2750)
12. Buchanan KA, Blackman AV, Moreau AW, Elgar D, Costa RP, Lalanne T, Tudor Jones AA, Oyrer J, Sjöström PJ. 2012 Target-specific expression of presynaptic NMDA receptors in neocortical microcircuits. *Neuron* **75**, 451–466. (doi:10.1016/j.neuron.2012.06.017)
13. Siegel SJ, Brose N, Janssen WG, Gasic GP, Jahn R, Heinemann SF, Morrison JH. 1994 Regional, cellular, and ultrastructural distribution of *N*-methyl-D-aspartate receptor subunit 1 in monkey hippocampus. *Proc. Natl Acad. Sci. USA* **91**, 564–568. (doi:10.1073/pnas.91.2.564)
14. Jourdain P *et al.* 2007 Glutamate exocytosis from astrocytes controls synaptic strength. *Nat. Neurosci.* **10**, 331–339. (doi:10.1038/nn1849)
15. Farb CR, Aoki C, Ledoux JE. 1995 Differential localization of NMDA and AMPA receptor subunits in the lateral and basal nuclei of the amygdala: a light and electron microscopic study. *J. Comp. Neurol.* **362**, 86–108. (doi:10.1002/cne.903620106)
16. Petralia RS, Yokotani N, Wenthold RJ. 1994 Light and electron microscope distribution of the NMDA receptor subunit NMDAR1 in the rat nervous system using a selective anti-peptide antibody. *J. Neurosci.* **14**, 667–696.
17. Bidoret C, Ayon A, Barbour B, Casado M. 2009 Presynaptic NR2A-containing NMDA receptors implement a high-pass filter synaptic plasticity rule. *Proc. Natl Acad. Sci. USA* **106**, 14 126–14 131. (doi:10.1073/pnas.0904284106)
18. Rossi B, Ogden D, Llano I, Tan YP, Marty A, Collin T. 2012 Current and calcium responses to local activation of axonal NMDA receptors in developing cerebellar molecular layer interneurons. *PLoS ONE* **7**, e39983. (doi:10.1371/journal.pone.0039983)
19. Liu H, Wang H, Sheng M, Jan LY, Jan YN, Basbaum AI. 1994 Evidence for presynaptic *N*-methyl-D-aspartate receptors in the spinal cord dorsal horn. *Proc. Natl Acad. Sci. USA* **91**, 8383–8387. (doi:10.1073/pnas.91.18.8383)
20. Lu CR, Hwang SJ, Phend KD, Rustioni A, Valtschanoff JG. 2003 Primary afferent terminals that express presynaptic NR1 in rats are mainly from myelinated, mechanosensitive fibers. *J. Comp. Neurol.* **460**, 191–202. (doi:10.1002/cne.10632)
21. Berretta N, Jones RS. 1996 Tonic facilitation of glutamate release by presynaptic *N*-methyl-D-aspartate autoreceptors in the entorhinal cortex. *Neuroscience* **75**, 339–344. (doi:10.1016/0306-4522(96)00301-6)
22. Sjöström PJ, Turrigiano GG, Nelson SB. 2003 Neocortical LTD via coincident activation of presynaptic NMDA and cannabinoid receptors. *Neuron* **39**, 641–654. (doi:10.1016/S0896-6273(03)00476-8)
23. Braiser DJ, Feldman DE. 2008 Synapse-specific expression of functional presynaptic NMDA receptors in rat somatosensory cortex. *J. Neurosci.* **28**, 2199–2211. (doi:10.1523/JNEUROSCI.3915-07.2008)
24. Mameli M, Carta M, Partridge LD, Valenzuela CF. 2005 Neurosteroid-induced plasticity of immature synapses via retrograde modulation of presynaptic NMDA receptors. *J. Neurosci.* **25**, 2285–2294. (doi:10.1523/JNEUROSCI.3877-04.2005)
25. Humeau Y, Shaban H, Bissière S, Lüthi A. 2003 Presynaptic induction of heterosynaptic associative plasticity in the mammalian brain. *Nature* **426**, 841–845. (doi:10.1038/nature02194)
26. Glitsch M, Marty A. 1999 Presynaptic effects of NMDA in cerebellar Purkinje cells and interneurons. *J. Neurosci.* **19**, 511–519.
27. Duguid IC, Smart TG. 2004 Retrograde activation of presynaptic NMDA receptors enhances GABA release at cerebellar interneuron–Purkinje cell synapses. *Nat. Neurosci.* **7**, 525–533. (doi:10.1038/nn1227)

28. Huang H, Bordey A. 2004 Glial glutamate transporters limit spillover activation of presynaptic NMDA receptors and influence synaptic inhibition of Purkinje neurons. *J. Neurosci.* **24**, 5659–5669. (doi:10.1523/JNEUROSCI.1338-04.2004)
29. Fiszman ML, Barberis A, Lu C, Fu Z, Erdélyi F, Szabó G, Vicini S. 2005 NMDA receptors increase the size of GABAergic terminals and enhance GABA release. *J. Neurosci.* **25**, 2024–2031. (doi:10.1523/JNEUROSCI.4980-04.2005)
30. Glitsch MD. 2008 Calcium influx through *N*-methyl-D-aspartate receptors triggers GABA release at interneuron–Purkinje cell synapse in rat cerebellum. *Neuroscience* **151**, 403–409. (doi:10.1016/j.neuroscience.2007.10.024)
31. Xue JG, Masuoka T, Gong XD, Chen KS, Yanagawa Y, Law SK, Konishi S. 2011 NMDA receptor activation enhances inhibitory GABAergic transmission onto hippocampal pyramidal neurons via presynaptic and postsynaptic mechanisms. *J. Neurophysiol.* **105**, 2897–2906. (doi:10.1152/jn.00287.2010)
32. Suárez LM, Suárez F, Del Olmo N, Ruiz M, González-Escalada JR, Solís JM. 2005 Presynaptic NMDA autoreceptors facilitate axon excitability: a new molecular target for the anticonvulsant gabapentin. *Eur. J. Neurosci.* **21**, 197–209. (doi:10.1111/j.1460-9568.2004.03832.x)
33. Samson RD, Paré D. 2005 Activity-dependent synaptic plasticity in the central nucleus of the amygdala. *J. Neurosci.* **25**, 1847–1855. (doi:10.1523/JNEUROSCI.3713-04.2005)
34. Wozny C, Maier N, Schmitz D, Behr J. 2008 Two different forms of long-term potentiation at CA1–subiculum synapses. *J. Physiol.* **586**, 2725–2734. (doi:10.1113/jphysiol.2007.149203)
35. Roggenhofer E, Fidzinski P, Bartsch J, Kurz F, Shor O, Behr J. 2010 Activation of dopamine D1/D5 receptors facilitates the induction of presynaptic long-term potentiation at hippocampal output synapses. *Eur. J. Neurosci.* **32**, 598–605. (doi:10.1111/j.1460-9568.2010.07312.x)
36. Bardoni R, Torsney C, Tong CK, Prandini M, MacDermott AB. 2004 Presynaptic NMDA receptors modulate glutamate release from primary sensory neurons in rat spinal cord dorsal horn. *J. Neurosci.* **24**, 2774–2781. (doi:10.1523/JNEUROSCI.4637-03.2004)
37. Casado M, Isope P, Ascher P. 2002 Involvement of presynaptic *N*-methyl-D-aspartate receptors in cerebellar long-term depression. *Neuron* **33**, 123–130. (doi:10.1016/S0896-6273(01)00568-2)
38. Rodríguez-Moreno A, Paulsen O. 2008 Spike timing-dependent long-term depression requires presynaptic NMDA receptors. *Nat. Neurosci.* **11**, 744–745. (doi:10.1038/nn.2125)
39. Andrade-Talavera Y, Duque-Feria P, Paulsen O, Rodríguez-Moreno A. 2016 Presynaptic spike timing-dependent long-term depression in the mouse hippocampus. *Cereb. Cortex* **26**, 3637–3654. (doi: 10.1093/cercor/bhw172)
40. Lien C-C, Mu Y, Vargas-Caballero M, Poo M-M. 2006 Visual stimuli-induced LTD of GABAergic synapses mediated by presynaptic NMDA receptors. *Nat. Neurosci.* **9**, 372–380. (doi:10.1038/nn1649)
41. Christie JM, Jahr CE. 2008 Dendritic NMDA receptors activate axonal calcium channels. *Neuron* **60**, 298–307. (doi:10.1016/j.neuron.2008.08.028)
42. Christie JM, Jahr CE. 2009 Selective expression of ligand-gated ion channels in L5 pyramidal cell axons. *J. Neurosci.* **29**, 11 441–11 450. (doi:10.1523/JNEUROSCI.2387-09.2009)
43. Pugh JR, Jahr CE. 2011 NMDA receptor agonists fail to alter release from cerebellar basket cells. *J. Neurosci.* **31**, 16 550–16 555. (doi:10.1523/JNEUROSCI.3910-11.2011)
44. Takago H, Nakamura Y, Takahashi T. 2005 G protein-dependent presynaptic inhibition mediated by AMPA receptors at the calyx of Held. *Proc. Natl Acad. Sci. USA* **102**, 7368–7373. (doi:10.1073/pnas.0408514102)
45. Takahashi T, Forsythe ID, Tsujimoto T, Barnes-Davies M, Onodera K. 1996 Presynaptic calcium current modulation by a metabotropic glutamate receptor. *Science* **274**, 594–597. (doi:10.1126/science.274.5287.594)
46. Forsythe ID, Barnes-Davies M. 1993 The binaural auditory pathway: excitatory amino acid receptors mediate dual time-course excitatory postsynaptic currents in the rat medial nucleus of the trapezoid body. *Proc. R. Soc. Lond. B* **251**, 151–157. (doi:10.1098/rspb.1993.0022)
47. Paoletti P, Vergnano AM, Barbour B, Casado M. 2009 Zinc at the glutamatergic synapses. *Neuroscience* **158**, 126–136. (doi:10.1016/j.neuroscience.2008.01.061)
48. Takahashi T, Kajikawa Y, Tsujimoto T. 1998 G-protein-coupled modulation of presynaptic calcium currents and transmitter release by a $GABA_B$ receptor. *J. Neurosci.* **18**, 3138–3146.
49. Kajikawa Y, Saitoh N, Takahashi T. 2001 GTP-binding protein $\beta\gamma$ subunits mediate presynaptic calcium current inhibition by $GABA_B$ receptor. *Proc. Natl Acad. Sci. USA* **98**, 8054–8058. (doi:10.1073/pnas.141031298)
50. Leão RM, von Gersdorff H. 2002 Noradrenaline increases high-frequency firing at the calyx of Held synapse during development by inhibiting glutamate release. *J. Neurophysiol.* **87**, 2297–2306.
51. Kimura M, Saitoh N, Takahashi T. 2003 Adenosine A1 receptor-mediated presynaptic inhibition at the calyx of Held of immature rats. *J. Physiol.* **553**, 415–426. (doi:10.1113/jphysiol.2003.048371)
52. Mizutani H, Hori T, Takahashi T. 2006 5-HT1B receptor-mediated presynaptic inhibition at the calyx of Held of immature rats. *Eur. J. Neurosci.* **24**, 1946–1954. (doi:10.1111/j.1460-9568.2006.05063.x)
53. Takahashi T, Hori T, Kajikawa Y, Tsujimoto T. 2000 The role of GTP-binding protein activity in fast central synaptic transmission. *Science* **289**, 460–463. (doi:10.1126/science.289.5478.460)
54. Casado M, Dieudonné S, Ascher P. 2000 Presynaptic N-methyl-D-aspartate receptors at the parallel fiber–Purkinje cell synapse. *Proc. Natl Acad. Sci. USA* **97**, 11 593–11 597. (doi:10.1073/pnas.200354297)
55. Bouvier, G. *et al.* 2016 Burst-dependent bidirectional plasticity in the cerebellum is driven by presynaptic NMDA receptors. *Cell Rep.* **15**, 104–116. (doi:10.1016/j.celrep.2016.03.004)
56. Kunz PA, Roberts AC, Philpot BD. 2013 Presynaptic NMDA receptor mechanisms for enhancing spontaneous neurotransmitter release. *J. Neurosci.* **33**, 7762–7769. (doi:10.1523/JNEUROSCI.2482-12.2013)
57. Kushmerick C, Price GD, Taschenberger H, Puente N, Renden R, Wadiche JI, Duvoisin RM, Grandes P, von Gersdorff H. 2004 Retroinhibition of presynaptic Ca^{2+} currents by endocannabinoids released via postsynaptic mGluR activation at a calyx synapse. *J. Neurosci.* **24**, 5955–5965. (doi:10.1523/JNEUROSCI.0768-04.2004)
58. von Gersdorff H, Schneggenburger R, Weis S, Neher E. 1997 Presynaptic depression at a calyx synapse: the small contribution of metabotropic glutamate receptors. *J. Neurosci.* **17**, 8137–8846.
59. Cuttle MF, Tsujimoto T, Forsythe ID, Takahashi T. 1998 Facilitation of the presynaptic calcium current at an auditory synapse in rat brainstem. *J. Physiol.* **512**, 723–729. (doi:10.1111/j.1469-7793.1998.723bd.x)
60. Ishikawa T, Kaneko M, Shin HS, Takahashi T. 2005 Presynaptic N-type and P/Q-type Ca^{2+} channels mediating synaptic transmission at the calyx of Held of mice. *J. Physiol.* **568**, 199–209. (doi:10.1113/jphysiol.2005.089912)
61. Renden R, Taschenberger H, Puente N, Rusakov DA, Duvoisin R, Wang LY, Lehre KP, von Gersdorff H. 2005 Glutamate transporter studies reveal the pruning of metabotropic glutamate receptors and absence of AMPA receptor desensitization at mature calyx of Held synapses. *J. Neurosci.* **25**, 8482–8497. (doi:10.1523/JNEUROSCI.1848-05.2005)
62. Min R, Nevian T. 2012 Astrocyte signaling controls spike timing-dependent depression at neocortical synapses. *Nat. Neurosci.* **15**, 746–753. (doi:10.1038/nn.3075)
63. Nevian T, Sakmann B. 2006 Spine Ca^{2+} signaling in spike-timing-dependent plasticity. *J. Neurosci.* **26**, 11 001–11 013. (doi:10.1523/JNEUROSCI.1749-06.2006)
64. Letellier M, Park YK, Chater TE, Chipman PH, Gautam SG, Oshima-Takago T, Goda Y. 2016 Astrocytes regulate heterogeneity of presynaptic strengths in hippocampal networks. *Proc. Natl Acad. Sci. USA* **113**, E2685–E2694. (doi:10.1073/pnas.1523717113)
65. Futai K, Okada M, Matsuyama K, Takahashi T. 2001 High-fidelity transmission acquired via a developmental decrease in NMDA receptor expression at an auditory synapse. *J. Neurosci.* **21**, 3342–3349.
66. Steinert JR, Postlethwaite M, Jordan MD, Chernova T, Robinson SW, Forsythe ID. 2010 NMDAR-mediated EPSCs are maintained and accelerate in time course during maturation of mouse and rat auditory brainstem *in vitro*. *J. Physiol.* **588**, 447–463. (doi:10.1113/jphysiol.2009.184317)

67. Cochilla AJ, Alford S. 1999 NMDA receptor-mediated control of presynaptic calcium and neurotransmitter release. *J. Neurosci.* **19**, 193–205.
68. Hsu S-H, Augustine G, Jackson M. 1996 Adaptation of Ca^{2+}-triggered exocytosis in presynaptic terminal. *Neuron* **17**, 501–512. (doi:10.1016/S0896-6273(00)80182-8)
69. Awatramani GB, Price GD, Trussell LO. 2005 Modulation of transmitter release by presynaptic resting potential and background calcium levels. *Neuron* **48**, 109–121. (doi:10.1016/j.neuron.2005.08.038)
70. Hori T, Takahashi T. 2009 Mechanisms underlying short-term modulation of transmitter release by presynaptic depolarization. *J. Physiol.* **587**, 2987–3000. (doi:10.1113/jphysiol.2009.168765)
71. Borst JG, Sakmann B. 1996 Calcium influx and transmitter release in a fast CNS synapse. *Nature* **383**, 431–434. (doi:10.1038/383431a0)
72. Issacson JS. 1998 $GABA_B$ receptor-mediated modulation of presynaptic currents and excitatory transmission at a fast central synapse. *J. Neurophysiol.* **80**, 1571–1576.
73. Ishii T *et al.* 1993 Molecular characterization of the family of *N*-methyl-D-aspartate receptor subunits. *J. Biol. Chem.* **268**, 2836–2843.
74. Herman MA, Jahr CE. 2007 Extracellular glutamate concentration in hippocampal slice. *J. Neurosci.* **27**, 9736–9741. (doi:10.1523/JNEUROSCI.3009-07.2007)
75. Durand GM, Bennett MVL, Zukin BS. 1993 Splice variants of the *N*-methyl-D-aspartate receptor NR1 identity domains involved in regulation by polyamines and protein kinase C. *Proc. Natl Acad. Sci. USA* **90**, 6731–6735. (doi:10.1073/pnas.90.14.6731)
76. Yamashita T, Kanda T, Eguchi K, Takahashi T. 2009 Vesicular glutamate filling and AMPA receptor occupancy at the calyx of Held synapse of immature rats. *J. Physiol.* **587**, 2327–2339. (doi:10.1113/jphysiol.2008.167759)
77. Cavelier P, Attwell D. 2005 Tonic release of glutamate by a DIDS-sensitive mechanism in rat hippocampal slices. *J. Physiol.* **564**, 397–410. (doi:10.1113/jphysiol.2004.082131)
78. Jonas P, Sakmann B. 1992 Glutamate receptor channels in isolated patches from CA1 and CA3 pyramidal cells of rat hippocampal slices. *J. Phyisol.* **455**, 143–171. (doi:10.1113/jphysiol.1992.sp019294)
79. Clements JD, Lester RA, Tong G, Jahr CE, Westbrook GL. 1992 The time course of glutamate in the synaptic cleft. *Science* **258**, 1498–1501. (doi:10.1126/science.1359647)
80. Iijima T, Iijima C, Iwao Y, Sankawa H. 2000 Difference in glutamate release between retina and cerebral cortex following ischemia. *Neurochem. Int.* **36**, 221–224. (doi:10.1016/S0197-0186(99)00119-9)
81. Kushmerick C, Renden R, von Gersdorff H. 2006 Physiological temperatures reduce the rate of vesicle pool depletion and short-term depression via an acceleration of vesicle recruitment. *J. Neurosci.* **26**, 1366–1377. (doi:10.1523/JNEUROSCI.3889-05.2006)